Electronic Supplementary Information

Computational study of the Fenton reaction at different pH ranges

Hsiu-Feng Lu,[a] Hui-Fen Chen,[b] Chai-Lin Kao,[b] Ito Chao[a] and Hsing-Yin Chen*[b]
[a]Institute of Chemistry, Academia Sinica, Taipei 11529, Taiwan
[b]Department of Medicinal and Applied Chemistry, Kaohsiung Medical University, Kaohsiung 80708, Taiwan

E-mail: hychen@kmu.edu.tw

Table of Contents

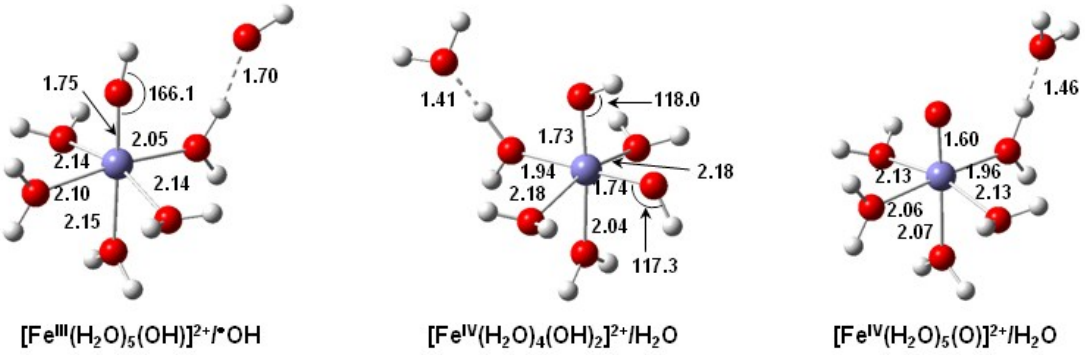

Fig. S1. B3LYP-D3/6-31++G** optimized structures of the three key intermediates in the Fenton reaction.

Linear regression of pK_a and ΔG_{deprot}

Table S1. CPCM-PBE0-D3/6-31+G* deprotonation free energies (kcal/mol) and experimental pK_a's for aqueous transition metal ions.

complex	ΔG_{deprot}	pK_a	Ref.
$[Mn^{III}(H_2O)_6]^{3+}$	229.3	0.08	a
$[Fe^{III}(H_2O)_6]^{3+}$	240.2	2.2	a
$[Sc^{III}(H_2O)_6]^{3+}$	245.7	4.3	b
$[(\mathbf{H}_2O)_5Fe^{III}(OH)]^{2+}$	259.4	6.33	c
$[Cu^{II}(H_2O)_6]^{2+}$	267.5	8	d,e
$[Fe^{II}(H_2O)_6]^{2+}$	274.6	9.5	a
$[Mn^{II}(H_2O)_6]^{2+}$	279.2	10.8	a,d

Ref. a. *Inorg. Chem. 35*, 4694–4702, **1996**. Ref. b. *J. Am. Chem. Soc. 121*, 3234–3235, **1999**. Ref. c. *Inorg. Chem. 38*, 603–605, **1999**. Ref. d. *Aquatic Chemistry: Chemical Equilibria and Rates in Natural Water*, 3rd ed.; John Wiley & Sons: New York, **1996**. Ref. e. *Hydrolysis of Cations; Robert E*; Krieger Publishing Company: Malabar, FL, **1976**.

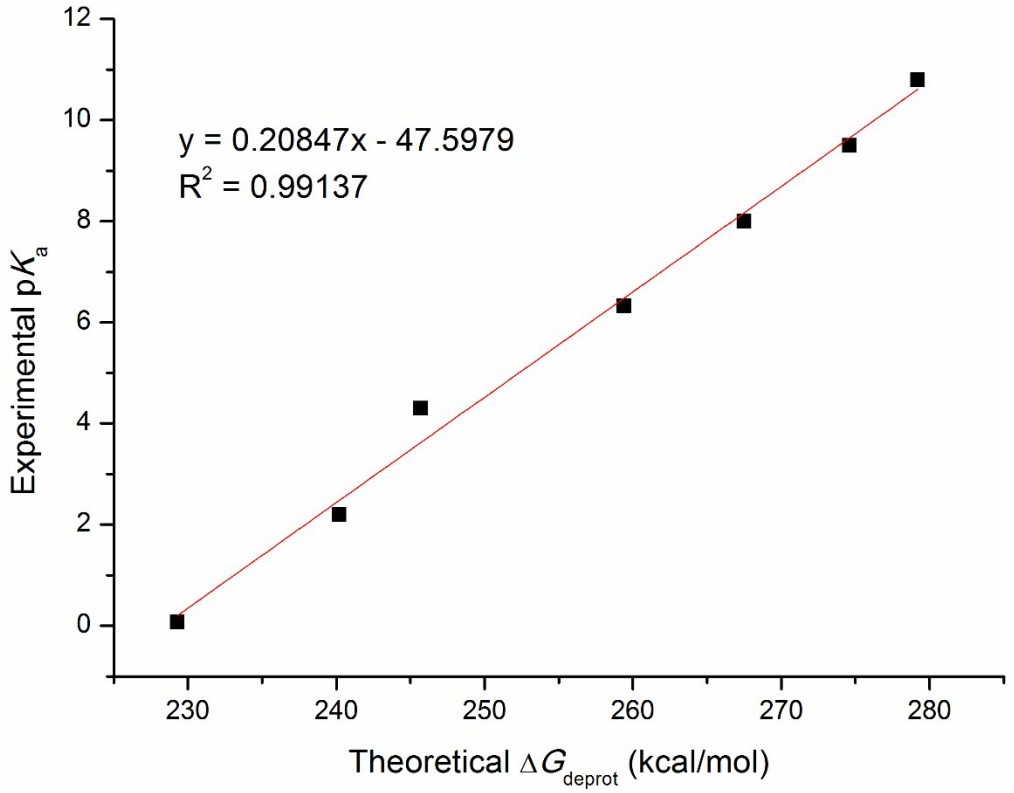

Fig. S2. Plot of linear regression between experimental pK_a and theoretical ΔG_{deprot}.

Table S2. Theoretical pK_a's estimated by using linear equation pK_a = 0.20847ΔG_{deprot} – 47.59790.

complex	ΔG_{deprot}	pK_a(theor.)	pK_a(expt.)	Ref.
$[Ti^{III}(H_2O)_6]^{3+}$	237.1	1.8	2.15	a
$[V^{III}(H_2O)_6]^{3+}$	242.7	3.0	2.6	b
$[Cr^{III}(H_2O)_6]^{3+}$	246.9	3.9	3.7	c
$[Co^{II}(H_2O)_6]^{2+}$	274.3	9.6	9.7	c
$[Co^{III}(H_2O)_6]^{3+}$	229.2	0.2	0.5	c
$[Ni^{II}(H_2O)_6]^{2+}$	273.8	9.5	9.9	d
$[V^{IV}(O)(H_2O)_5]^{2+}$	256.7	5.9	5.3-6.0	e–i

Ref. (a) *J. Chem. Soc., Dalton Trans.* 596–601, **1977**. (b) *Inorg. Chem.40*, 3101–3112, **2001**. (c) *J. Chem. Educ. 73*, 516–517, **1996**. (d) *Inorg. Chem. 46*, 7971–7981, **2007**. (e) *In Comprehensive Coordination Chemistry*; Wilkinson, G., Gillard, R. D., McCleverty, J. A., Eds.; Pergamon Press: New York, **1987**; Vol. 3. (f) *Inorg. Chem. 14*, 2860−2862, **1975**. (g) *J. Chem. Soc., Dalton Trans.* 1156−1159, **1973**. (h) *Acta Chem. Scand. 9*, 1177−1192, **1955**. (i) *An. Quim. 62B*, 123−193, **1966**.

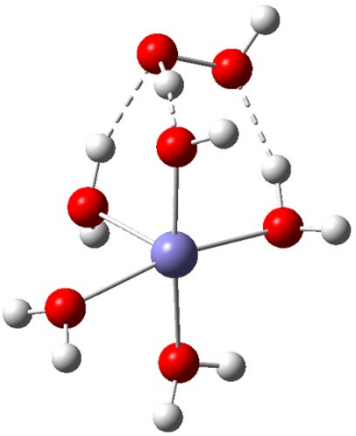

Fig. S3. CPCM-PBE0-D3/6-31+G* optimized structure for *cis*-$[(H_2O)_4Fe^{II}(OH)(H_2O_2)]^+$.

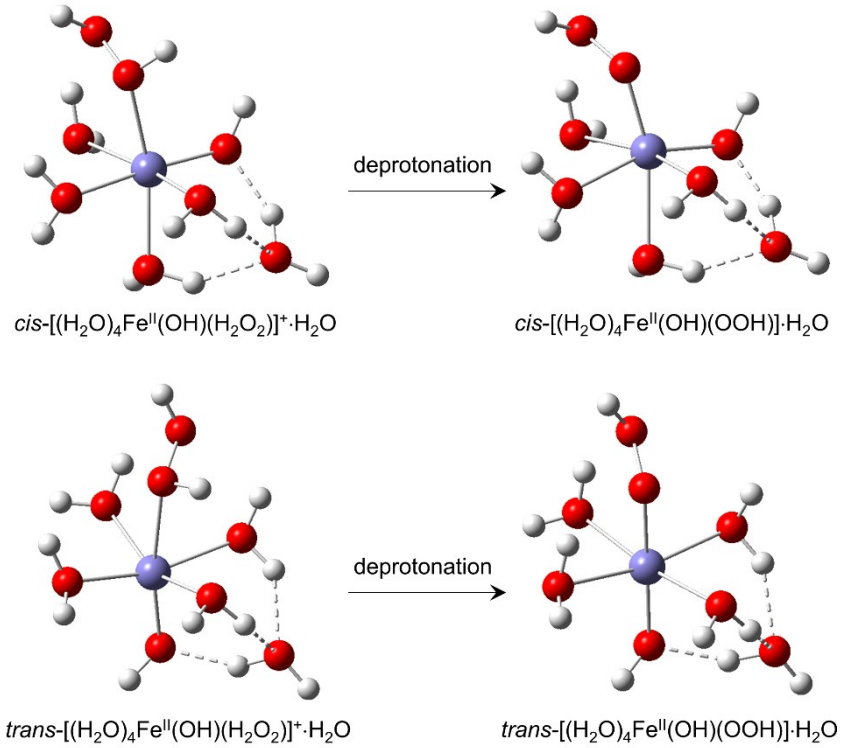

Fig. S4. CPCM-PBE0-D3/6-31+G* optimized structures for *cis*- and *trans*-$[(H_2O)_4Fe^{II}(OH)(H_2O_2)]^+\cdot H_2O$ and *cis*- and *trans*-$[(H_2O)_4Fe^{II}(OH)(OOH)]\cdot H_2O$.

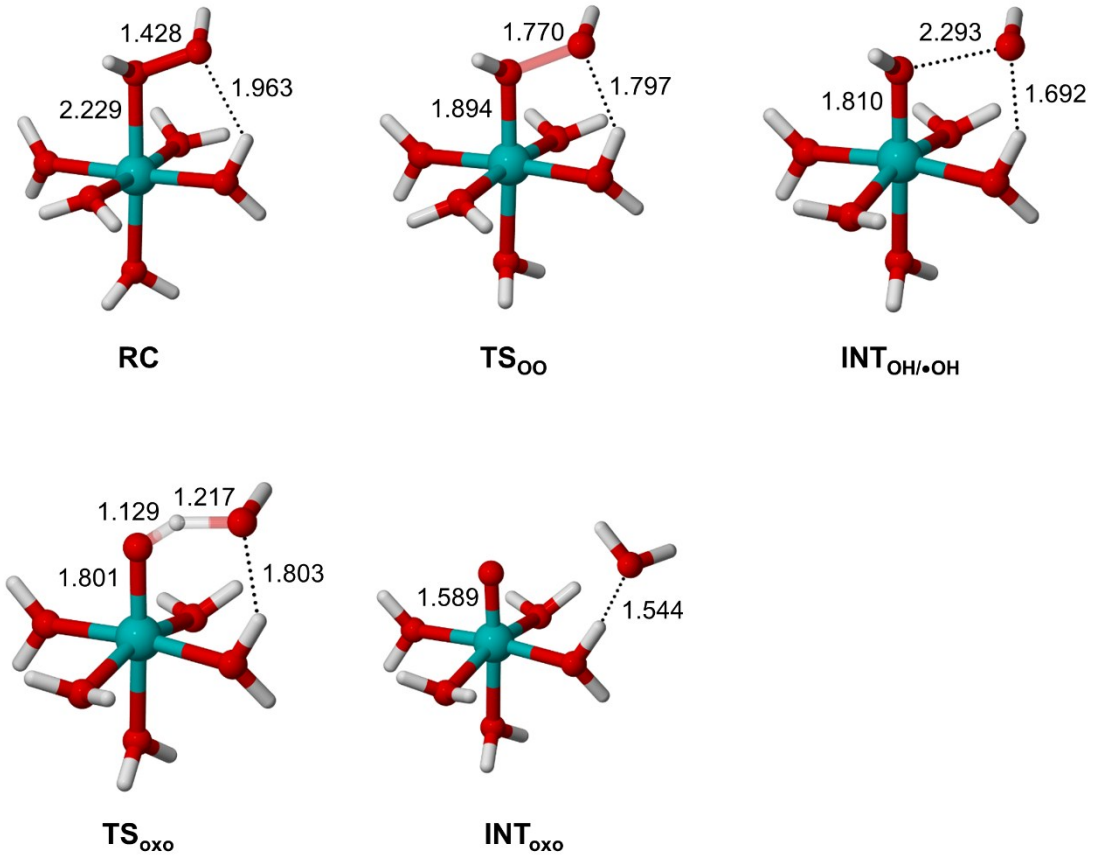

Fig. S5. CPCM-M06/6-31+G* optimized geometries of the reactant complex, intermediates, and transition states for the Fenton reaction starting from $[(H_2O)_5Fe^{II}(H_2O_2)]^{2+}$.

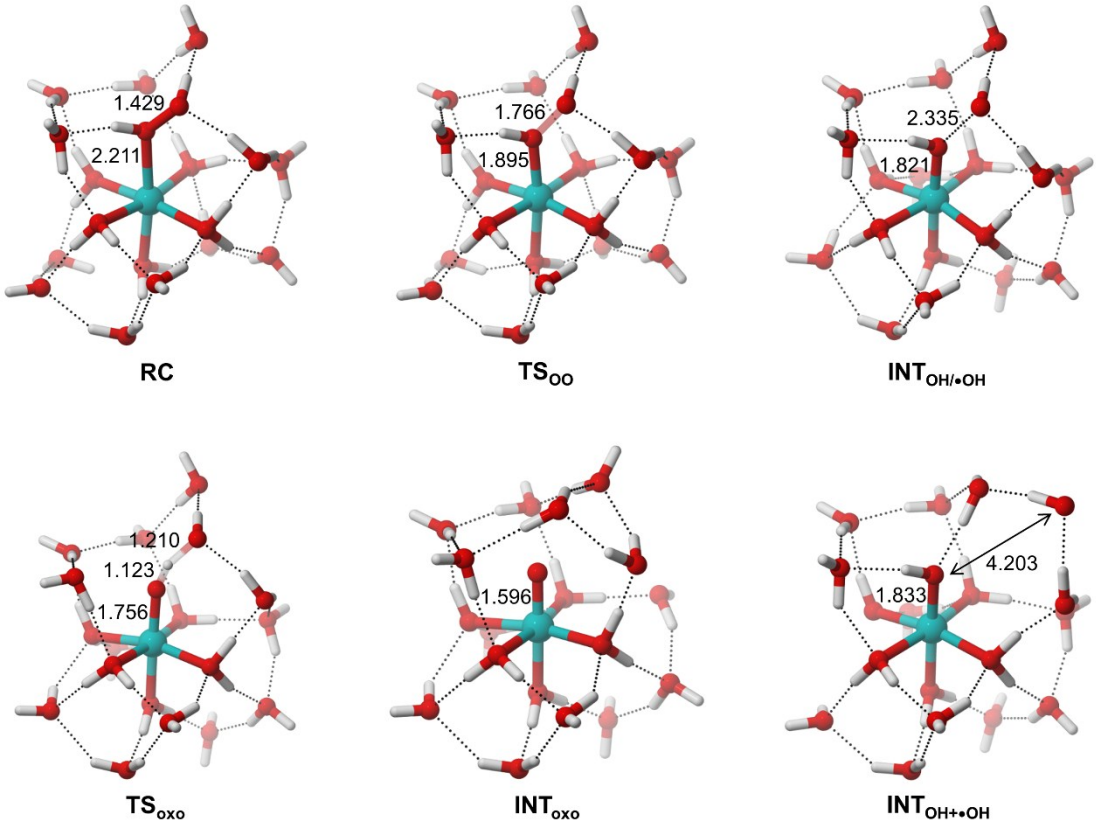

Fig. S6. CPCM-PBE0-D3/6-31+G* optimized geometries of the reactant complex, intermediates, and transition states for the Fenton reaction starting from $[(H_2O)_5Fe^{II}(H_2O_2)]^{2+}\cdot(H_2O)_{12}$.

Table S3. Relative free energies of Fenton reactions starting from reactant complexes $[(H_2O)_5Fe^{II}(H_2O_2)]^{2+}$, $[(H_2O)_5Fe^{II}(H_2O_2)]^{2+}\cdot(H_2O)_{12}$, and $[(H_2O)_5Fe^{II}(H_2O_2)]^{2+}\cdot H_3O^+(H_2O)_{12}$.[a]

$[(H_2O)_5Fe^{II}(H_2O_2)]^{2+}$					
method	**RC**	**TS_{OO}**	**$INT_{OH/\bullet OH}$**	**TS_{oxo}**	**INT_{oxo}**
PBE0-D3/6-31+G(d)	0.0	16.0	8.8	16.9	–3.3
PBE0-D3/Def2-TZVP	0.0	18.0	11.0	17.8	–0.6
PW6B95/6-31+G(d)	0.0	17.9	12.1	20.9	–1.0
$[(H_2O)_5Fe^{II}(H_2O_2)]^{2+}\cdot(H_2O)_{12}$					
method	**RC**	**TS_{OO}**	**$INT_{OH/\bullet OH}$**	**TS_{oxo}**	**INT_{oxo}**
PBE0-D3/6-31+G(d)	0.0	14.2	6.7	13.6	–3.8
PBE0-D3/Def2-TZVP	0.0	16.0	7.6	13.1	–1.2
PW6B95/6-31+G(d)	0.0	15.7	7.6	15.6	–3.9
$[(H_2O)_5Fe^{II}(H_2O_2)]^{2+}\cdot H_3O^+(H_2O)_{12}$					
method	**RC**	**$INT_{OH/\bullet OH}$**	**INT_{oxo}**	**$INT_{FeIII+\bullet OH}$**	
PBE0-D3/6-31+G(d)	0.0	1.6	–3.4	–3.6	
PBE0-D3/Def2-TZVP	0.0	2.9	–0.4	–2.7	
PW6B95/6-31+G(d)	0.0	5.3	–0.4	0.0	

[a]Geometry optimizations and vibrational frequencies for free energy corrections were carried out at PBE0-D3/6-31+G(d) level.

Table S4. Relative free energies of Fenton reactions starting from reactant complexes $[(H_2O)_5Fe^{II}(OOH)]^+$ and $[(H_2O)_5Fe^{II}(OOH)]^+\cdot(H_2O)_{12}$.[a]

$[(H_2O)_5Fe^{II}(OOH)]^+$					
method	**RC**	**TS_{OO}**	**$INT_{oxyl/\bullet OH}$**	**TS_{HAT}**	**$INT_{oxo\text{-}OH}$**
PBE0-D3/6-31+G(d)	0.0	14.3	13.3	12.8	–10.2
PBE0-D3/Def2-TZVP	0.0	16.2	15.5	14.4	–7.5
PW6B95/6-31+G(d)	0.0	16.2	15.9	16.1	–7.3
$[(H_2O)_5Fe^{II}(OOH)]^+\cdot(H_2O)_{12}$					
method	**RC**	**TS_{OO}**	**$INT_{oxyl/\bullet OH}$**	**TS_{HAT}**	**$INT_{oxo\text{-}OH}$**
PBE0-D3/6-31+G(d)	0.0	11.7	8.0	7.1	–7.7
PBE0-D3/Def2-TZVP	0.0	14.0	10.5	9.2	–4.4
PW6B95/6-31+G(d)	0.0	13.9	11.5	11.4	–5.5

[a]Geometry optimizations and vibrational frequencies for free energy corrections were carried out at PBE0-D3/6-31+G(d) level.

Table S5. Relative free energies of Fenton reactions starting from reactant complexes *trans*-$[(H_2O)_5Fe^{II}(OOH)(OH)]\cdot(H_2O)_{12}$ and *cis*-$[(H_2O)_5Fe^{II}(OOH)(OH)]\cdot(H_2O)_{12}$.[a]

trans-$[(H_2O)_5Fe^{II}(OOH)(OH)]\cdot(H_2O)_{12}$					
method	^{t}**RC**	^{t}**TS$_{OO}$**	^{t}**INT$_{oxyl/\bullet OH}$**	^{t}**TS$_{HAT}$**	^{t}**INT$_{oxo\text{-}diOH}$**
PBE0-D3/6-31+G(d)	0.0	11.6	5.1	4.7	–13.8
PBE0-D3/Def2-TZVP	0.0	13.7	7.7	7.0	–10.2
PW6B95/6-31+G(d)	0.0	14.1	9.5	9.3	–11.3
cis-$[(H_2O)_5Fe^{II}(OOH)(OH)]\cdot(H_2O)_{12}$					
method	^{c}**RC**	^{c}**TS$_{OO}$**	^{c}**INT$_{oxyl/\bullet OH}$**	^{c}**TS$_{HAT}$**	^{c}**INT$_{oxo\text{-}diOH}$**
PBE0-D3/6-31+G(d)	0.4	8.7	0.4	–1.0	–19.2
PBE0-D3/Def2-TZVP	0.3	10.4	2.6	0.8	–15.9
PW6B95/6-31+G(d)	0.6	10.2	3.5	2.6	–17.7

[a]Geometry optimizations and vibrational frequencies for free energy corrections were carried out at PBE0-D3/6-31+G(d) level.